Simultaneous Defocus Integration during Refractive Development

Dennis Y. Tse,[1] Carly S. Lam,[1] Jeremy A. Guggenheim,[2] Chuen Lam,[1] King-kit Li,[1] Quan Liu,[3] and Chi-ho To[1]

PURPOSE. To determine the effects of simultaneously presented myopic and hyperopic defocus on the refractive development of chicks.

METHODS. A novel form of dual-power lens was designed. Normal chicks 7 to 8 days of age were fitted with a dual-power lens over one eye and a plano lens over the fellow (control) eye. Dual-power lenses of $+20/-10$, $+10/-10$, $+5/-10$, and plano/-10-D were tested, along with $+10/-10$-D lenses having differing ratios (50:50, 33:67, and 25:75) of surface area devoted to each power. Ocular refraction and axial ocular component dimensions were assessed after 6 days of lens wear, by retinoscopy and high-frequency ultrasound, respectively. In a separate experiment designed to test the effect of dual-power lens wear on the refractive development of myopic eyes, chicks were fitted with a dual-power $+10/-10$-D lens for 6 days, after myopia had been induced by 6 days of -10-D lens wear.

RESULTS. For each of the dual-power lenses tested, the refractive end point of the treated eye was found to lie between the two optical powers of the lens (but with the response weighted in favor of the effect of myopic defocus). Refractive development appeared to be modulated by the sign, dioptric magnitude, and relative contribution (relative contrast) of the imposed optical defocuses through an integrative mechanism. Chicks with myopia induced by -10-D lens wear recovered when treated with a $+10/-10$-D dual-power lens.

CONCLUSIONS. The chick retina can discern both the sign and the magnitude of optical defocus. Chick eyes were able to integrate blur cues from simultaneously presented images focused either side of the photoreceptors and to modulate their refractive development accordingly. This implies that the complex nature of defocus in the visual environment may play a critical role in the pathogenesis of myopia. The results suggest a rational method for arresting or reversing the development of myopia, which may be useful in the treatment of human myopia if the primate retina is also capable of responding to simultaneously presented opposing defocus cues. (*Invest Ophthalmol Vis Sci.* 2007;48:5352–5359) DOI:10.1167/iovs.07-0383

Myopia typically occurs due to excessive enlargement of the eye, such that in the unaccommodated state an image is focused in front of, rather than onto, the photoreceptor layer of the retina. In recent years myopia has reached epidemic proportions in parts of East Asia, including China, Hong Kong, Japan, Singapore, and Taiwan, with up to 70% to 90% of 17- to 18-year-olds in the region affected.[1–5] Growing evidence suggests that the prevalence of myopia is increasing in the Caucasian populations in Australia and the United States as well.[6]

Myopia incurs more than a minor inconvenience, since high myopia is a leading cause of retinal degeneration[7] and visual impairment.[8] In fact, myopic degeneration is the second leading cause of low vision in Hong Kong[9] and is the fifth leading cause of blindness in the United States.[10] Optical aids are usually prescribed purely to correct refractive error and, at present, there is no proven clinical treatment for retarding myopia's progression.

Myopia is a multifactorial disorder. Twin and family studies indicate a genetic predisposition to myopia.[11] By contrast, epidemiology studies have shown that myopia is more prevalent in early adults than in older adults within a population that shares the same gene pool.[12–14] Therefore, environmental factors are strongly indicated in the recent epidemic of myopia.

Naturally occurring refractive errors (myopia and hyperopia) are scarce and small in magnitude among both wild and domesticated adult animals—for example, the pigeon,[15] chick,[16] tree shrew,[17] rhesus monkey,[18] fish,[19] marmoset,[20] and guinea pig.[21] This phenomenon of the scarcity of naturally occurring refractive errors is driven by the process of emmetropization: a robust homeostatic mechanism found in diverse species that guides postnatal eye growth (reviewed in Ref. 22). Refractive errors are common at birth; hence, images of distant objects are focused in front of the photoreceptors (myopic defocus) in some subjects and behind the photoreceptors (hyperopic defocus) in others. However, the growth of the component parts of the eye is carefully coordinated in such a way that, as the animal matures, the position of the photoreceptors becomes increasingly well matched to the combined focal length of the eye's refractive elements. Eventually, the eye becomes relatively free of refractive error (emmetropic) for targets at infinity. (In reality, this is a somewhat simplified view: hyperopia is more common than myopia in early infancy, and, in most populations, most individuals undergo emmetropization to a refractive state of low hyperopia rather than precise emmetropia.[16,18,21]) It is yet to be answered why children so commonly develop myopia if the dimensions of the eye are under homeostatic control to match its optical power. In fact, the exact mechanism of emmetropization remains to be unraveled, although it is known to operate largely locally within the eye and does not necessarily require innervation

from the central nervous system.[23] Experimentally, the emmetropization process can be manipulated by mounting ophthalmic lenses before the eyes of young animals and then monitoring the changes in refractive status and ocular dimensions. Results have shown that school work and other intensive close work are risk factors for myopia.[10,24] Emmetropization is known to be principally visually guided,[22] and therefore, intuitively, extreme environments such as predominantly close reading distance may somehow upset the natural balance of visual input for normal eye growth.

Previous studies of reading habits,[25] accommodative stress reduction,[26,27] and lens-induced emmetropization have typically used relatively simple visual targets. However, visual scenes typically comprise multiple spatially distinct objects, forming images at a variety of levels of defocus. These rich spatial and temporal visual inputs may provide important cues to the emmetropization system. In this study, we tested the hypothesis that ocular growth is modulated by the integration of such differentially defocused images in the visual field.

METHODS

White leghorn chicks (*Gallus gallus*) were obtained and bred as SPF (specific pathogen free) fertilized eggs from SPAFAS India (Venky's, Viththalwadi, Maharashtra, India). The chicks were housed in an enclosure made of fine metal mesh (to minimize restriction of distant viewing) under a 12-hour-light/12-hour-dark cycle of 450 lux (mea-
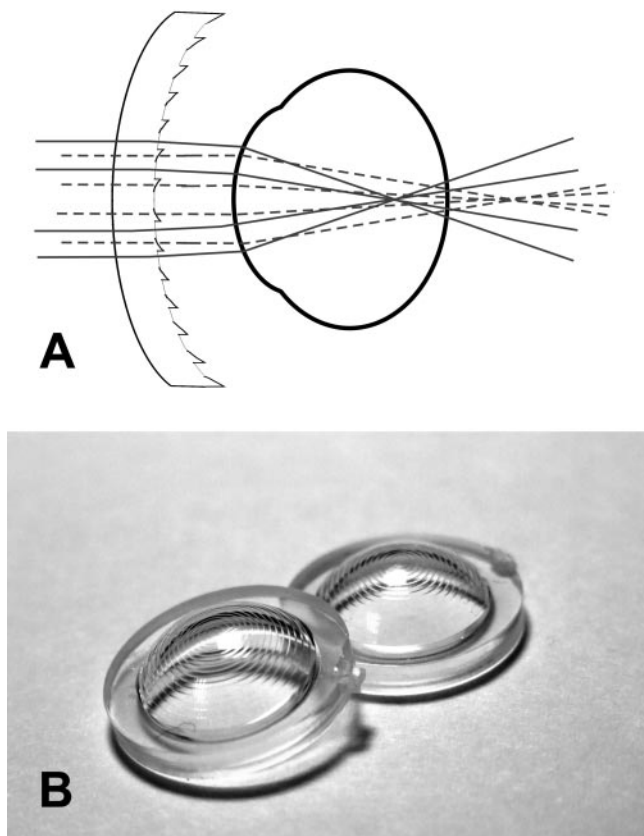
FIGURE 1. (A) In the unaccommodated eye, the dual-power lens produces two distinct foci, one in front of and the other behind the photoreceptors, introducing simultaneous myopic defocus and hyperopic defocus on the retina (diagram not drawn to scale). (B) Photograph of concentric dual-power lenses. Annuli of equal width are evenly distributed in the 11-mm optical zone, thus minimizing the effect of pupil size on the ratio of myopic and hyperopic defocus and extending the angle of view from center to periphery.
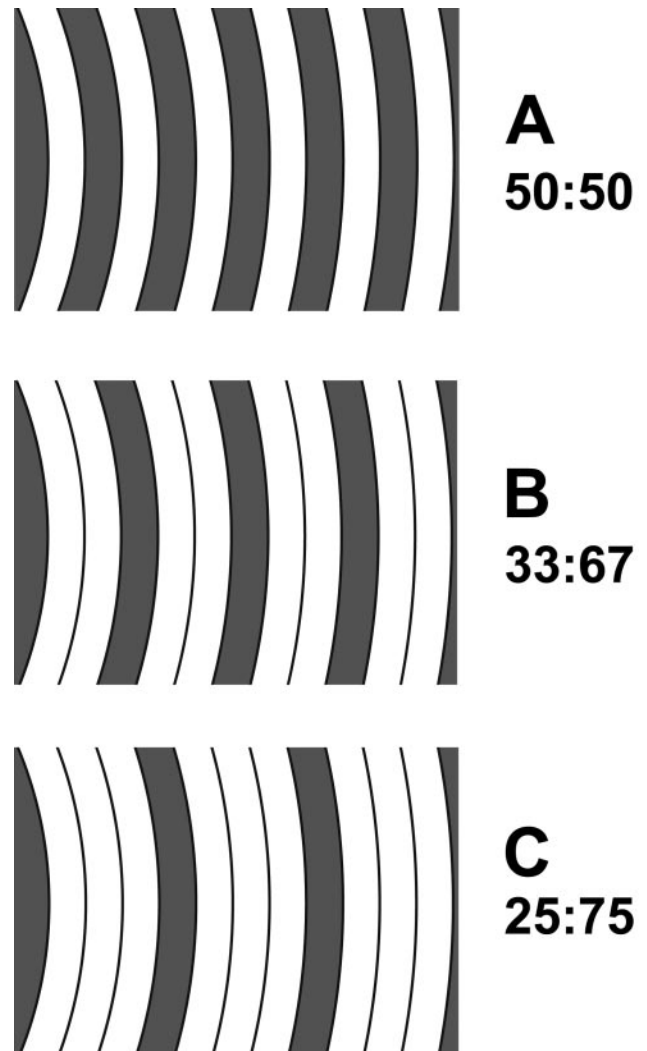
FIGURE 2. Diagram showing how the annuli on the lenses are arranged to provide different ratios (in area) of contributing powers. *Shaded regions*: annuli of +10 D. *White regions*: annuli of −10 D. (A) The 50:50 area lens. Each +10-D annulus is coupled with one −10-D annulus. (B) The 33:67 area lens. Each +10-D annulus is coupled with two consecutive −10-D annuli. (C) The 25:75 area lens. Each +10-D annulus is coupled with three consecutive −10-D annuli.

sured at the level of the food containers) and given food and water ad libitum. All chicks were 7 to 8 days old at the start of lens wear experiments. All the rearing and experimental procedures were approved by The Hong Kong Polytechnic University's Animal Ethics Committee and were in compliance with the ARVO Statement for the Use of Animals in Ophthalmic and Visual Research.

Dual-Power Lens System

Lenses were attached with the aid of Velcro rings glued to the feathers around the eye.[28] Dual-power lenses (Fig. 1) designed with an optical design program (Zemax; Zemax Design Corp., Bellevue, WA) based on the Fresnel principle were optimized to minimize spherical aberrations. Lenses were manufactured from PMMA by cast molding. All lenses had an optical zone diameter of 11 mm and an anterior radius of curvature of 6.68 mm. The posterior surface comprised a series of annuli of different radii of curvature. The pitch width of each annulus was 0.4 mm for the +10/−10-D (50:50 area) dual-power lens and 0.1 mm for the other powers. Between each annulus, there was a transition curve 0.005 mm in width. The number of annuli for the 33:67 (area) and the 25:75 (area) lenses

Table 1. Interocular Difference in Refractive Error in Response to Monocular Dual-Power (or Control) Lens Wear in Chicks

Treatment Lens Power (D)	*n*	Day*	Interocular Difference in Refractive Error† (D)	Statistical Significance‡	
Experiment 1					
+20/−10	10	6	13.5 ± 0.7	*P* < 0.01	*P* < 0.01
+10/−10	10	6	4.7 ± 0.4	*P* < 0.01	*P* < 0.01
+5/−10	10	6	−0.6 ± 0.5	*P* < 0.01	*P* < 0.01
Plano/−10	10	6	−3.9 ± 0.6	*P* < 0.01	*P* < 0.01
+20	11	6	17.1 ± 0.8	Ref.	—
+10	11	6	9.7 ± 0.4	Ref.	—
+5	10	6	4.5 ± 0.4	Ref.	—
Plano	11	6	−0.3 ± 0.3	Ref.	—
−10	15	6	−11.1 ± 0.3	—	Ref.
Experiment 2					
50:50	10	6	4.7 ± 0.4	Ref.	*P* < 0.01
33:66	11	6	−6.7 ± 0.6	*P* < 0.01	*P* < 0.01
25:75	10	6	−9.3 ± 0.8	*P* < 0.01	*P* > 0.05
0:100	15	6	−11.1 ± 0.3	*P* < 0.01	Ref.
Experiment 3. Group A					
—	10	0	−0.2 ± 0.1	Ref.	—
+10/−10	10	2	1.5 ± 0.6	*P* < 0.05	—
+10/−10	10	4	3.9 ± 0.7	*P* < 0.01	—
+10/−10	10	6	3.9 ± 0.6	*P* < 0.01	Ref.
−10	9	8	−1.8 ± 0.7	—	*P* > 0.01
−10	5	10	−6.0 ± 2.3	—	*P* < 0.01
−10	5	12	−8.2 ± 1.7	—	*P* < 0.01
Experiment 3. Group B					
—	13	0	−0.1 ± 0.1	Ref.	—
−10	13	2	−5.7 ± 0.5	*P* > 0.01	—
−10	13	4	−8.3 ± 0.6	*P* < 0.01	—
−10	13	6	−10.1 ± 0.6	*P* < 0.01	Ref.
+10/−10	8	8	−6.3 ± 1.6	—	*P* < 0.05
+10/−10	8	10	−2.1 ± 1.5	—	*P* < 0.01
+10/−10	7	12	0.4 ± 1.2	—	*P* < 0.01

Ref., reference group.
* Treatment duration (in days) when measurements were obtained.
† Mean ± SE.
‡ Difference from corresponding reference group.

was 52—for example, the +10/−10-D (25:75 area) lens contained 13 annuli of positive power and 39 annuli of negative power. The extent of the field of view through the optical zones of the dual-power lenses was approximately 150°. Thus, the lenses would produce overlying images, focused in different planes, over the central and midperipheral retina. It should be noted that the dual-power lenses would *not* produce concentric rings of hyperopic and myopic defocus on the retina. Figure 2 shows a schematic diagram of the distribution of annuli for the different lens types.

Ocular refraction was measured to ±0.50 D by retinoscopy and trial lenses in the two principal meridians (usually at axes 90 and 180). Spherical equivalent power was calculated by averaging the refractive powers of the two meridians. Axial ocular dimensions were measured using a high-frequency A-scan ultrasound system with a 30-MHz polymer transducer sampled at 100 MHz.[28] All measurements were made with the animals under isoflurane anesthesia in gaseous oxygen so that accommodation was relaxed during both refraction and axial length measurements without the use of additional cycloplegic drugs. Data are presented as the mean ± SE. Statistics were performed with ANOVA and the Bonferroni post hoc test (SPSS, Chicago, IL). The number of animals in each group is shown in Table 1. Part of the data in this work have been published in abstract form (Tse DY et al. *IOVS* 2005;46:ARVO E-Abstract 1974).

## Experiment 1: Simultaneous Myopic Defocus and Hyperopic Defocus

In the first experiment, we simultaneously imposed both myopic and hyperopic defocus on one eye of young chicks and studied how

the emmetropization system integrated these disparate growth cues. The simultaneous myopic and hyperopic defocus was achieved by using custom-designed and manufactured dual-power lenses, which took the form of concentric annuli of alternating power. These lenses simultaneously introduced overlapping optical images that in an unaccommodated eye would be focused on either side of the retina. Chicks wore a plano (zero power) lens over the fellow eye as a control. Lenses were cleaned at least once every 2 days. More frequent cleaning was unnecessary, since eyes covered with plano lenses did not develop myopia. For comparison, additional groups of chicks were raised wearing a single vision lens (+20, +10, +5, plano, or −10 D) over one eye and a plano lens over the fellow eye. The four dual-power treatment groups were processed and measured together in a series of experiment, whereas the five single-vision control groups were processed and measured together in another series.

Experiment 2: Increasing Lens Area for Hyperopic Defocus

To further characterize the integration of competing defocus cues, we varied the relative proportions of the myopic and hyperopic defocus annuli of dual-power lenses, from the 50:50 contribution examined in experiment 1. Because the effect of myopic defocus outweighed the effect of hyperopic defocus for various power combinations in experiment 1, the lens area generating myopic defocus was decreased. Two dual-power lenses (+10/−10 D) with increasing proportions of hyperopic defocus were produced: a
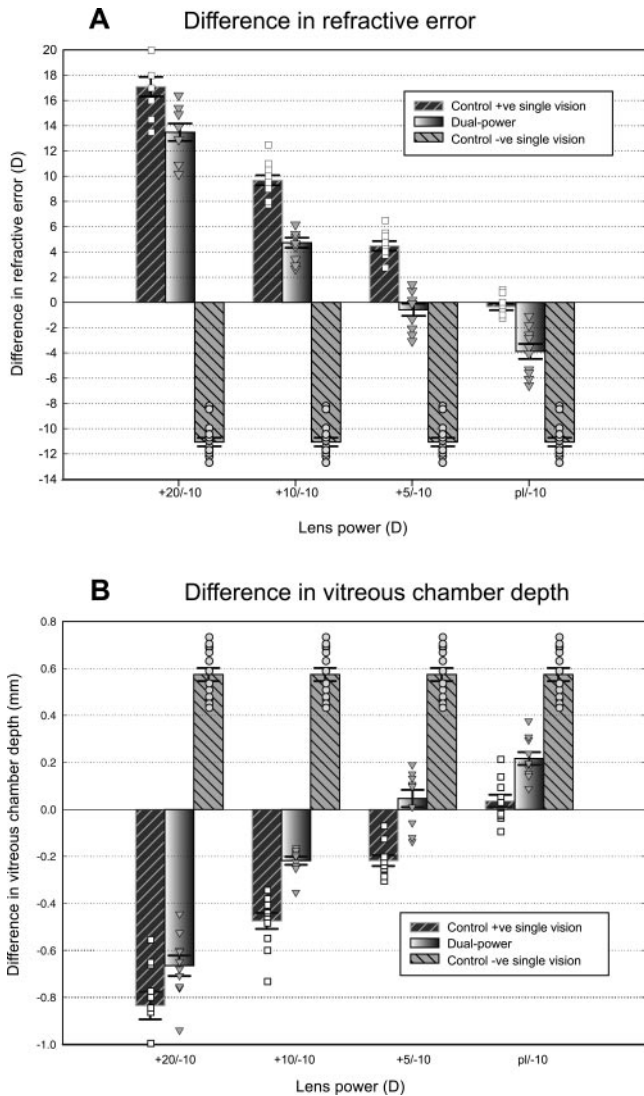
FIGURE 3. The interocular difference (treated eye minus control eye) in refractive error (**A**) and VCD (**B**) after 6 days of monocular treatment-lens wear. *Hatched bars*: the means for animal groups wearing dual-power lenses of +20/−10, +10/−10, +5/−10 and 0/−10 D (all with a 50:50 ratio of positive-to-negative annuli). *Dark gray bars*: the mean for control animal groups wearing monocular single-vision positive (or plano) lenses of power: +20, +10, +5, and 0 D. *Light gray bars*: the mean for the control animal groups wearing monocular negative single-power lenses (−10 D). Note that the results for a single −10-D control group are depicted alongside each treatment group to facilitate comparison. Error bars, SE. *Squares*, *inverted triangles*, and *circles*: individual data points. The differences in refractive error and VCD of all dual-power groups were significantly different from the corresponding single-vision controls. *P* < 0.01 for all comparisons, with the exception of the +20/−10-D and the plano/−10-D groups, in which the interocular differences in VCD were significantly different from the +20 D and plano controls (*P* < 0.05; ANOVA and Bonferroni post hoc tests).

33:67 lens (i.e., 33% of +10 D and 67% of −10 D) and a 25:75 lens. The effects of these lenses were compared with those of the 50:50 (+10/−10 D) dual-power lens and the 0:100 (−10-D) single-vision lens used in Experiment 1.

Experiment 3: Effect of a Switch from a Negative Single-Vision Lens to a Dual-Power Lens and Vice Versa

To investigate the effect of simultaneous defocus in eyes with an existing refractive error, we performed a crossover experiment in which either a

−10-D single-vision lens or a +10/−10-D (50:50) dual-power lens was worn on one eye for 6 days (stage 1), followed by a further 6 days in which the −10-D lens was replaced by a +10/−10-D lens, and vice versa (stage 2). The fellow eye of all chicks was fitted with a plano lens throughout the 12 days of the experiment as a control.

RESULTS

Experiment 1: Integration of Competing Myopic and Hyperopic Defocus during Emmetropization

As reported in previous studies, rearing chicks with a single-vision lens altered their refractive state in such a manner as to
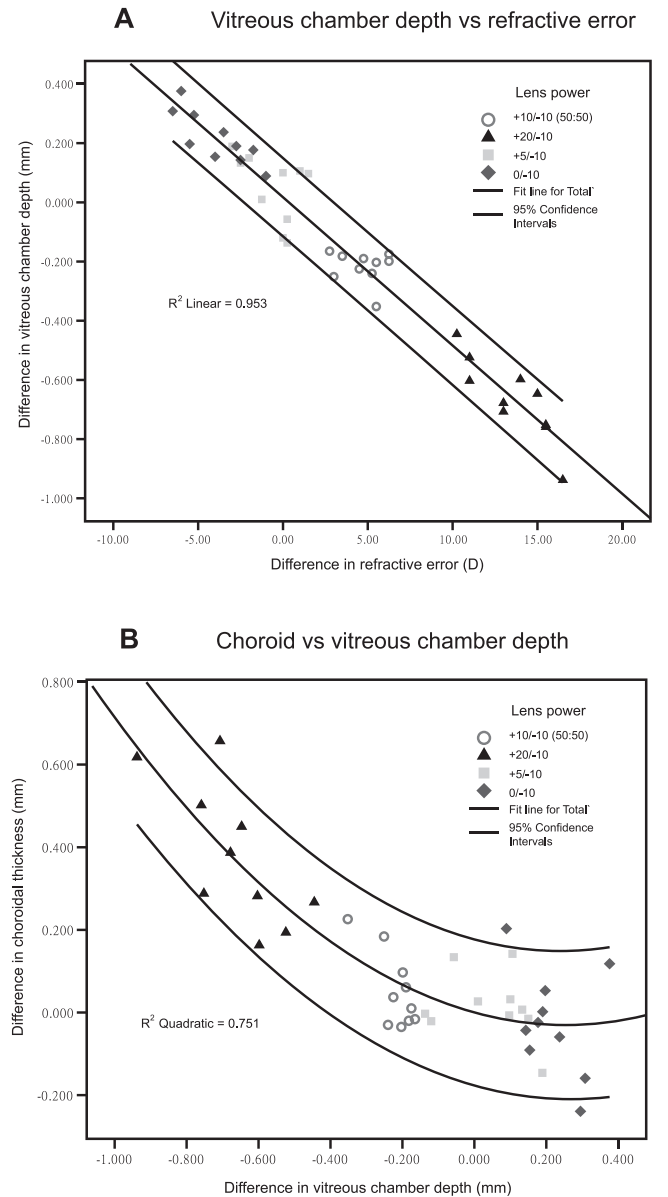
FIGURE 4. Scatterplots of interocular difference in VCD versus (**A**) refractive error and (**B**) choroidal thickness and after 6 days of dual-power lens wear. The strong linear relationship between interocular differences in refractive error and VCD was consistent with most of the change in refractive error being attributable to the change in VCD. The relationship between the interocular difference in VCD and the interocular difference in choroidal thickness was best fitted with a quadratic equation, indicating that the thickness of choroid was only partially responsible for the change in VCD of treated eyes. Structural changes to the sclera are thus implicated.
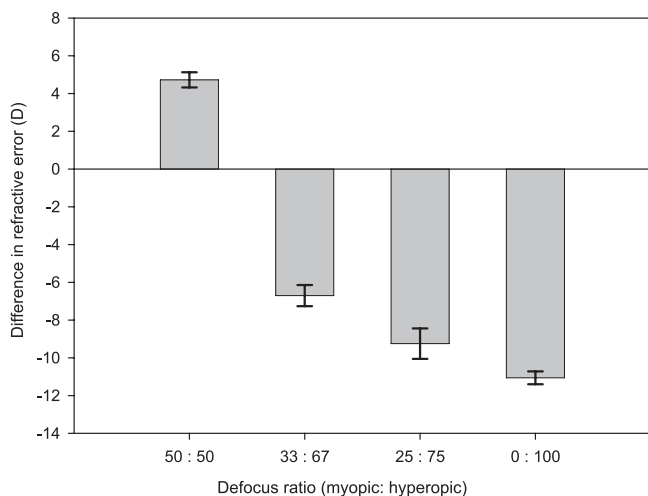
FIGURE 5. The interocular difference in refractive error at day 6 for different ratios of +10/−10-D defocus. The 33:67 group was significantly different from the 50:50, 25:75, and 0:100 groups ($P < 0.01$, $P < 0.05$, and $P < 0.01$ respectively; in post hoc analysis). The 25:75 group showed a relatively high SE compared with that in the other groups and was not significantly different from the 0:100 group ($P > 0.05$).

compensate for the imposed defocus (compensation was complete for the lower lens powers tested and partial for higher lens powers; Fig. 3). In stark contrast, the refractive state of chicks reared with dual-power lenses was not altered to match either of the two planes of induced defocus: Instead, the refractive end point of the eye fell between the two optical powers of the lens (the resultant refractive error was: +13.5, +4.7, −0.6, and −3.9 D; for dual-power lenses of: +20/−10, +10/−10, +5/−10, and 0/−10 D, respectively; Fig. 3A). The refractive end points were significantly different from the two powers of the dual-power lens and the respective single-vision control lenses in all cases (ANOVA, Bonferroni post hoc, $P < 0.01$). Of interest, the refractive end point of dual-power-lens–wearing eyes was always slightly more positive than the numerical mean of the two lens powers.

Ocular biometry using high-resolution A-scan ultrasonography demonstrated that the major structural correlate to the refractive changes just described was a change in the interocular vitreous chamber depth (VCD). The interocular differences in VCD between the treated and fellow control eyes were: −0.665, −0.218, 0.047, and 0.217 mm, for dual lenses with powers: +20/−10, +10/−10, +5/−10, and 0/−10 D, respectively (Fig. 3B). These changes correlated highly with the differences in refractive error between the two eyes ($R = 0.97$, $P < 0.01$; Fig. 4A). Changes in choroidal thickness also contributed to the refractive compensation to the dual-power lenses (eyes with shorter VCDs had thicker choroids, whereas there was no apparent thinning of the choroid when VCD increased; Fig. 4B). The interocular difference in refractive error was stable after 6 days of dual-power lens wear (data not shown). Thus, even though the treated eyes were still exposed to continuous competing defocuses, they exhibited no further change in refraction relative to control eyes.

Experiment 2: Effects of the Relative Extent of Competing Defocus

After 6 days of lens wear, the interocular difference in refractive error was +4.7, −6.7, and −9.3 D for chicks wearing 50:50, 33:67, and 25:75 ratio dual-power lenses, respectively, and −11.1 D for chicks wearing −10-D single vision lenses (Fig. 5). The refractive end points were significantly shifted
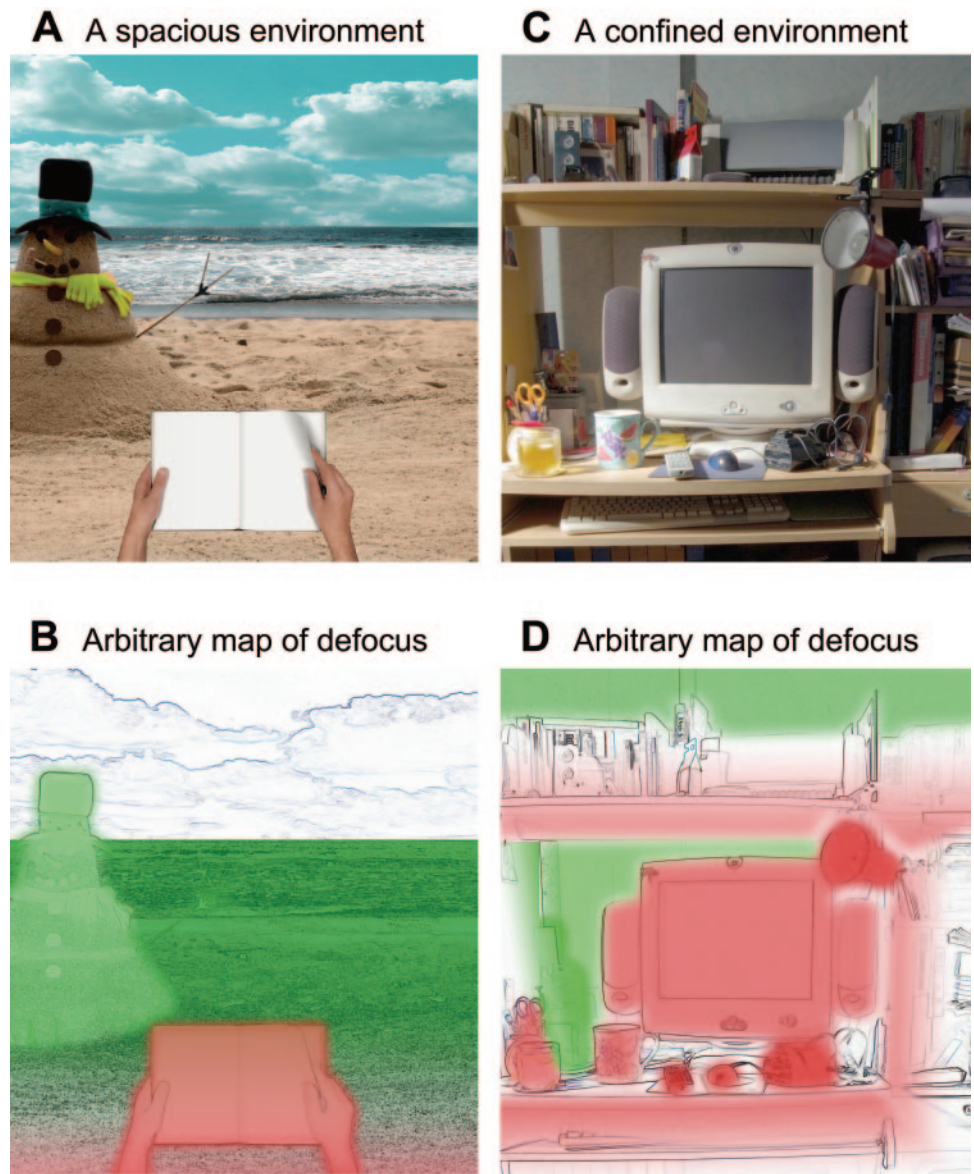
toward myopia when the ratio of the two powers decreased from 50:50 to 33:67 or lower ($P < 0.01$), and the refractive error of the 33:67 group was significantly different from that of the 0:100 control ($P < 0.01$). These ratio-dependent responses further suggest that visual processing in the retina integrates simultaneous defocus information concerning the relative contribution (relative contrast) of the defocus, as well as its sign and dioptric magnitude.

Experiment 3: Effect of Simultaneous Defocus on Existing Myopia

Refraction and ocular biometry were performed every 2 days to monitor the time course of the response (Fig. 6). As found in experiment 1, eyes wearing a dual-power lens in stage 1 grew to become slightly hyperopic relative to their fellow control eyes (+3.9 D, $n = 10$). The refractive error of the eyes tended to stabilize between days 4 and 6, but then became myopic during stage 2 when fitted with a −10-D lens. Eyes wearing a −10-D single vision lens during stage 1 became markedly myopic (−10.1 D, $n = 13$). However, after switching to a dual-power lens type (stage 2), they recovered such that they approached emmetropia (0.4 D; $n = 7$) after 6 days. We were not able to follow the refractive changes beyond 12 days, because by this age the lenses tended to fall off repeatedly, and so it is not yet clear whether refractive errors were stable by this point.
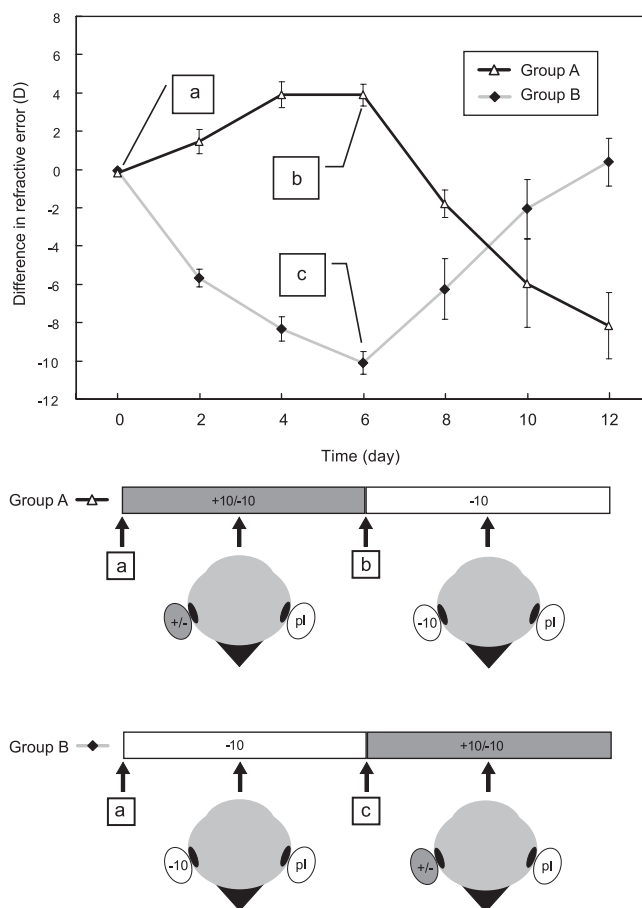
FIGURE 6. Interocular difference in refractive error versus time in the lens-switching experiment. (a) First day of treatment, (b) +10/−10-D dual-power lens switched to −10-D single vision lens, (c) −10-D single vision lens switched to +10/−10-D dual-power lens. Error bars, SE. The treatment groups are shown in the cartoon.

A A spacious environment

C A confined environment

B Arbitrary map of defocus

D Arbitrary map of defocus

FIGURE 7. Visual environments characterizing different profiles of simultaneous defocus. (**A**) Example of a spacious outdoor reading environment. The subject adopts a frontal reading posture. (**B**) Map of optical defocus distribution for (**A**). Saturation of the colors represents relative strength of defocus. (**C**) Example of a confined indoor working environment. (**D**) Map of optical defocus distribution for (**C**). Saturation of the colors represents relative strength of defocus. (**B**, **D**) *Green*: myopic defocus; *magenta*: hyperopic defocus.

DISCUSSION

It has been hypothesized that the eye uses the average amount of blur against sharp vision to signal growth toward myopia until emmetropia is achieved.[29] According to this hypothesis, the simultaneous myopic and hyperopic defocus experienced by chicks in our study would lead the treated eye to grow increasingly myopic. Our results provide evidence against this notion and suggest that emmetropization is jointly modulated by the sign, dioptric magnitude, and relative contribution (relative contrast) of defocus. The interaction was somewhat additive: We found myopic defocus to be more potent than hyperopic defocus in modulating eye growth. A similar bias toward myopic defocus has been noted during intermittent lens wear[30] and lens-switching experiments,[31] in which competing-defocus stimuli were presented sequentially. The results of experiment 2 suggest that the integration of simultaneous competing defocus information is also influenced by the relative contribution of the two focal powers (i.e., their relative contrast on the retina). Since the final refractive error of eyes wearing +10/−10-D lenses was hyperopic for 50:50 ratio lenses, yet myopic for 33:67 lenses, a ratio between these two values is likely to balance the competing inputs to produce emmetropia.

That eyes can integrate competing defocus information temporally[31] suggests not only that the eye can acquire and integrate optical cues, but also that information concerning prior defocus exposure is somehow retained (perhaps either as a chemical message with a particular half-life,[32] or through some form of synaptic plasticity[33]). Our results expand on this notion, by suggesting that the retina can integrate opposing defocus signals even when they are presented simultaneously. Of particular interest was the fact that refractive development stabilized (Fig. 6, point b) with the retina at a position between the two planes of defocus, where no sharp image would be obtained in the unaccommodated eye. Presumably, at this point, the emmetropization system is at an equilibrium in which the opposing inputs are balanced. Thus, our results are consistent with the idea that "stop" and "go" signals may play a role in emmetropization.[34]

The physiological mechanisms underlying the decoding of retinal defocus are far from clear, although there is evidence that image decoding may occur at the level of retinal amacrine

cells.[35] One possibility is that the single layer of photoreceptors functions as a multiple-channel system. For example, in the presence of longitudinal chromatic aberration, the different chromatic channels of cone photoreceptors may function like a series of sensors located at different positions along the optical axis[19] and contribute to decoding the sign of defocus (although it is difficult to imagine how this could be achieved without knowledge of the spectral composition of the light source). Another hypothesis contends that the dioptric distance between the image and the photoreceptor layer may not be stationary, but rather that accommodation microfluctuations associated with the arterial pulse[36] and/or the instantaneous heart rate[37] create movement of the image plane relative to the photoreceptor layer. Thus, temporal sampling of photoreceptor outputs may provide information analogous to a multiplane sensor series. If the visual system uses several strategies to guide emmetropization, then previous attempts to remove a single optical cue may have been confounded by the use of the others.[38]

All the refractive and biometric measurements performed in the present study were made "on axis." However, recent experiments[39,40] (Morgan IG et al. *IOVS* 2006;47:ARVO E-Abstract 3328) suggest that peripheral defocus may play an important role in regulating global, as well as local, refractive development. More work is needed to elucidate the degree of peripheral defocus in chicks viewing through dual-power lenses, and to what extent, if any, this contributes to refractive development along the optical axis.

This work raises two important questions. First, as pointed out by Flitcroft et al. (*IOVS* 2006;47:ARVO E-Abstract 4778), since the natural visual environment exposes the eye to an ever-changing scene comprising multiple levels of simultaneous defocus (Fig. 7), how is all this complexity decoded to modulate emmetropization? Second, since in chicks, dual-power, competing-defocus lenses can guide myopic eyes toward emmetropia, do similar methods hold promise for treating children with myopia?

Acknowledgments

References

1. Lam CS, Goldschmidt E, Edwards MH. Prevalence of myopia in local and international schools in Hong Kong. *Optom Vis Sci.* 2004;81:317–322.
2. Lin LL, Shih YF, Hsiao CK, Chen CJ, Lee LA, Hung PT. Epidemiologic study of the prevalence and severity of myopia among schoolchildren in Taiwan in 2000. *J Formos Med Assoc.* 2001;100:684–691.
3. Matsumura H, Hirai H. Prevalence of myopia and refractive changes in students from 3 to 17 years of age. *Surv Ophthalmol* 1999;44(suppl 1):S109–S115.
4. Saw SM, Tong L, Chua WH, et al. Incidence and progression of myopia in Singaporean school children. *Invest Ophthalmol Vis Sci.* 2005;46:51–57.
5. Zhao J, Pan X, Sui R, Munoz SR, Sperduto RD, Ellwein LB. Refractive error study in children: results from Shunyi district, China. *Am J Ophthalmol.* 2000;129:427–435.
6. Rose K, Smith W, Morgan I, Mitchell P. The increasing prevalence of myopia: implications for Australia. *Clin Exp Ophthalmol.* 2001;29:116–120.
7. Pierro L, Camesasca FI, Mischi M, Brancato R. Peripheral retinal changes and axial myopia. *Retina.* 1992;12:12–17.
8. Avila MP, Weiter JJ, Jalkh AE, Trempe CL, Pruett RC, Schepens CL. Natural history of choroidal neovascularization in degenerative myopia. *Ophthalmology.* 1984;91:1573–1581.
9. Yap M, Cho J, Woo G. A survey of low vision patients in Hong Kong. *Clin Exp Optom.* 1990;73:19–22.
10. Curtin BJ. *The Myopias. Basic Science and Clinical Management.* Philadelphia: Harper & Row; 1985.
11. Goss DA, Wickham MG. Retinal-image mediated ocular growth as a mechanism for juvenile onset myopia and for emmetropization: a literature review. *Doc Ophthalmol.* 1995;90:341–375.
12. Goh WS, Lam CS. Changes in refractive trends and optical components of Hong Kong Chinese aged 19–39 years. *Ophthalmic Physiol Opt.* 1994;14:378–382.
13. Lam CS, Goh WS, Tang YK, Tsui KK, Wong WC, Man TC. Changes in refractive trends and optical components of Hong Kong Chinese aged over 40 years. *Ophthalmic Physiol Opt.* 1994;14:383–388.
14. Morgan I, Rose K. How genetic is school myopia? *Prog Retin Eye Res.* 2005;24:1–38.
15. Fitzke FW, Hayes BP, Hodos W, Holden AL. Electrophysiological optometry using Scheiner's principle in the pigeon eye. *J Physiol.* 1985;369:17–31.
16. Irving EL, Sivak JG, Curry TA, Callender MG. Chick eye optics: zero to fourteen days. *J Comp Physiol [A].* 1996;179:185–194.
17. Marsh-Tootle WL, Norton TT. Refractive and structural measures of lid-suture myopia in tree shrew. *Invest Ophthalmol Vis Sci.* 1989;30:2245–2257.
18. Smith EL 3rd, Hung LF. The role of optical defocus in regulating refractive development in infant monkeys. *Vision Res.* 1999;39:1415–1435.
19. Kroger RH, Wagner HJ. The eye of the blue acara (Aequidens pulcher, Cichlidae) grows to compensate for defocus due to chromatic aberration. *J Comp Physiol [A].* 1996;179:837–842.
20. Troilo D, Nickla DL, Wildsoet CF. Choroidal thickness changes during altered eye growth and refractive state in a primate. *Invest Ophthalmol Vis Sci.* 2000;41:1249–1258.
21. Howlett MH, McFadden SA. Emmetropization and schematic eye models in developing pigmented guinea pigs. *Vision Res.* 2007;47:1178–1190.
22. Wallman J, Winawer J. Homeostasis of eye growth and the question of myopia. *Neuron.* 2004;43:447–468.
23. Wildsoet CF, Schmid KL. Optical correction of form deprivation myopia inhibits refractive recovery in chick eyes with intact or sectioned optic nerves. *Vision Res.* 2000;40:3273–3282.
24. Zadnik K, Mutti DO. Prevalence of myopia. In: Rosenfield M, Gilmartin B, eds. *Myopia and Nearwork.* Oxford, UK: Butterworth-Heinemann; 1998.
25. Hepsen IF, Evereklioglu C, Bayramlar H. The effect of reading and near-work on the development of myopia in emmetropic boys: a prospective, controlled, three-year follow-up study. *Vision Res.* 2001;41:2511–2520.
26. Edwards MH, Li RW, Lam CS, Lew JK, Yu BS. The Hong Kong progressive lens myopia control study: study design and main findings. *Invest Ophthalmol Vis Sci.* 2002;43:2852–2858.
27. Gwiazda J, Hyman L, Hussein M, et al. A randomized clinical trial of progressive addition lenses versus single vision lenses on the progression of myopia in children. *Invest Ophthalmol Vis Sci.* 2003;44:1492–1500.
28. Wildsoet C, Wallman J. Choroidal and scleral mechanisms of compensation for spectacle lenses in chicks. *Vision Res.* 1995;35:1175–1194.
29. Norton TT, Siegwart JT Jr. Animal models of emmetropization: matching axial length to the focal plane. *J Am Optom Assoc.* 1995;66:405–414.
30. Schmid KL, Wildsoet CF. Effects on the compensatory responses to positive and negative lenses of intermittent lens wear and ciliary nerve section in chicks. *Vision Res.* 1996;36:1023–1036.
31. Winawer J, Zhu X, Choi J, Wallman J. Ocular compensation for alternating myopic and hyperopic defocus. *Vision Res.* 2005;45:1667–1677.
32. Wallman J. Retinal control of eye growth and refraction. In: Osborne NN, Chader GJ, eds. *Progress in Retinal Research.* Oxford, UK: Pergamon Press; 1993:133–153.

33. Guggenheim JA. The "LTP-hypothesis" of retinal image sampling in emmetropisation. *Ophthalmic Physiol Opt*. 1998;18:379.

34. Rohrer B, Stell WK. Basic fibroblast growth factor (bFGF) and transforming growth factor beta (TGF-beta) act as stop and go signals to modulate postnatal ocular growth in the chick. *Exp Eye Res*. 1994;58:553–561.

35. Fischer AJ, McGuire JJ, Schaeffel F, Stell WK. Light- and focus-dependent expression of the transcription factor ZENK in the chick retina. *Nat Neurosci*. 1999;2:706–712.

36. Winn B, Pugh JR, Gilmartin B, Owens H. Arterial pulse modulates steady-state ocular accommodation. *Curr Eye Res*. 1990;9:971–975.

37. Collins M, Davis B, Wood J. Microfluctuations of steady-state accommodation and the cardiopulmonary system. *Vision Res*. 1995;35:2491–2502.

38. Wildsoet CF, Howland HC, Falconer S, Dick K. Chromatic aberration and accommodation: their role in emmetropization in the chick. *Vision Res*. 1993;33:1593–1603.

39. Schippert R, Schaeffel F. Peripheral defocus does not necessarily affect central refractive development. *Vision Res*. 2006;46:3935–3940.

40. Smith EL 3rd, Kee CS, Ramamirtham R, Qiao-Grider Y, Hung LF. Peripheral vision can influence eye growth and refractive development in infant monkeys. *Invest Ophthalmol Vis Sci*. 2005;46:3965–3972.

E R R A T U M

Erratum in: "Diagnosis of Plus Disease in Retinopathy of Prematurity Using Retinal Image multiScale Analysis" by Gelman et al. (*Invest Ophthalmol Vis Sci*. 2005;46:4734–4738.)

In the third paragraph of the Methods, the fourth sentence should read, "Normalized vectors T1 and T2 are formed by points along the skeleton (Fig. 2a), and the angle (θ) between each pair of vectors is obtained by computing the arccosine of their dot product."